Simulation Study of An Interleaved Flyback Converter for Micro Grid Systems Operating in the CCM Mode

Metin SALİHMUHSİN (msalihmuhsin@ksu.edu.tr)
Kahramanmaraş Sütçü İmam University

Research Article

Keywords: Interleaved Flyback Converter, Micro grid, PV Panel, PI Controller, Matlab/Simulink

Posted Date: June 13th, 2023

DOI: https://doi.org/10.21203/rs.3.rs-3029097/v1

Abstract

This paper presents a design and an implementation of an isolated grid connected micro inverter system that is based on an interleaved flyback topology. The developed system gets input from a 250 W PV panel, converts the dc energy into ac and connects it to the grid. This work covers the simulation aspect of developing the above mentioned system where extensive simulations are performed in order to find and optimize values of desired parameters and simulate the overall system. The CCM (Continues Conduction Mode) of operation for the flyback converter is preferred as it generates considerably less amount of the current ripple at converter output when compared to DCM operation and less amount of power loss. A feedback loop with a PI controller is incorporated into the design in order to properly stabilize the system. Simulation results demonstrated that the developed system generates sinusoidal voltage and current signals of 50 Hz in frequency with desired amplitudes at the output of the system. Connection of generated ac waveforms to the grid is accomplished by means of a PLL block. THD of the grid current is found as 11.57% due to spikes at zero crossings.

I. INTRODUCTION

Utilization of the power generation system that depend on solar energy in both industrial and residential areas has greatly increased in recent years due to its being a renewable and clean source of energy. These systems have proven to be reliable over years, as they require small maintenance fees and cause no danger to the nature. Taking into consideration that the life expectancy of PV panels with today's technology well excees 25 years and solar energy is available at almost everywhere, usage of the micro grid systems is expected to increase in the future.

Micro grids are small-sized energy generating units in which energy is obtained from mostly renewable sources such as the solar or wind energy and then converted into grid frequency ac energy which is either directly utilized by the local network or supplied to the grid. There have been numerous studies in order to improve the cost and efficiency

of such systems and develop optimum design for them in recent years [1–26]. Tamyurek and Kirimer [19] developed a low cost micro grid system with interleaved flyback topology where the dc energy obtained from PV panels is converted into sinusoidal ac energy and connected to the grid. Both PLECS (Piecewise Linear Electrical Circuit Simulation) and Simulink are used to generate models of their system. DCM (Discontinuous Conduction Mode) operation of the converter is preferred in order to achieve fast dynamic response and guaranteed stability of the system operation. No feedback loop is utilized in their system other than the feedback block embedded in the PLL algorithm. Optimization of various design parameters was done using simulations. The experimental part of their work was accomplished by building and evaluating a small prototype of simulated system for 1 KW output power which is suitable to be used in small residential areas. By applying an MPPT technique based on perturb & observe algorithm, they had achieved 97% of PV panel efficiency with 86% inverter static efficiency. They have

reported a THD of 3.86% for the output current of the converter and close to unity power factor for their design.

As a continuation study of their earlier work, Tamyurek and Kirimer [20] increased the power level of their previously developed system to 2 KW by going through several design improvements. They have reported 90.16% inverter efficiency, 4.42% THD for grid current and 0.998 pf for their improved design. The DCM mode of the converter operation and the open loop control of the overall system were again preferred in this later design.

The goal of this study is to develop a simulation model of a micro grid system that obtains dc energy from a PV panel and converts it into an ac energy using the interleaved flyback converter in order to supply it to the grid. The CCM mode of operation is utilized in the flyback topology since it provides less ripple at the output current and leads to less power loss. In order to overcome the stability problem that might occur because of CCM mode of operation, a feedback loop with a PI controller is incorporated into the design. Matlab/Simulink software is used to calculate and optimize parameters of the model and perform simulation of the overall system. The following studies are performed in prior to this study by us in order to develop a proper background to this work [27–39].

The remaining parts of this work are organized as follows. Section 2 gives detailed description of each sub-block of the overall system including theoretical background for interleaved flyback topology. Section 3 provides implementation details of the developed Matlab/Simulink program. Section 4 demonstrates simulation results and discussions. Section 5 provides conclusion.

II. REPRESENTATION OF MICRO GRID WITH BLOCK DIAGRAMS

The proposed micro grid system is composed of several blocks. The first block is the PV Source block. The output of PV Source block is connected to Flyback block where the 2 stage interleaved flyback converter is implemented. This block is followed by an output capacitor and H bridge block. The output of H bridge block is a grid frequency sinusoidal waveform. Finally, these sinusoidally shaped voltage and current signals are synchronized and connected to the grid by means of a PLL block. The block diagram of the micro grid system is given in Fig. 1 and the schematic circuit of the system is provided in Fig. 2.

A. The PV Panel Block

The PV Panel block contains a model of the PV panel followed by an input line filter. The filter is used to eliminate high frequency harmonics and smooth out the current signal obtained from the PV panel. TDK CWT250-60P poly-crystalline PV panel specifications are used to simulate this

block in the simulation. The utilized PV panel has an output power of 250 W and consists of 60 serially connected PV cells. Each PV cell can be modeled by a schematic circuit given in Fig. 3.

There are 4 unknown parameters in this cell model that have to be calculated namely the photo current of the cell I_{ph}, the diode reverse saturation current I_o, the series resistance R_s, and the shunt resistance R_{sh}. Numerous methods are illustrated in literature in order to find these unknown parameters. In [27], we have developed a Matlab/Simulink program to calculate these 4 unknown parameters by implementing an accurate method chosen from the literature [22]. The developed program was then used to generate I-V and P-V curves of the PV panel which was shown to be very close to those provided by the manufacturer. Figure 4 shows I-V curves generated by the developed program and that provided by the manufacturer.

B. The Decoupling Capacitor Block

The decoupling capacitor placed in between the PV source and interleaved flyback converter acts as a buffer and helps to maintain constant dc voltage at PV terminals. In doing so, it provides a low impedance path for instantaneous demand that the PV source is subjected by the output of the converter which is tied to the grid or the load. The orientation and sizing of the decoupling capacitor are important in order to maintain low ripple at the PV terminals. Increasing amount of ripple at PV terminals yields proportional or even larger amount of increase in the value of THD of the output current. It's reported by Zengin et al [26] that the value of decoupling capacitor could be calculated based on the following formula based on certain assumptions.

$$C \geq \frac{I_{PV}}{(2\pi f_l)\Delta V_{PV}} \quad (1)$$

where ΔV_{PV} is peak to peak voltage ripple across the decoupling capacitor, I_{PV} is the average PV current and f_l is the line frequency.

C. Theoretical Background for Interleaved Flyback Converter

Although the interleaved flyback architecture used in this work has 2 flyback cells in parallel, the converters are operated in such a way that the PWM pulse signal applied to the switch S1 is shifted by 180^o and applied to the switch S2 during each switching period. Consequently, operations of the both flyback cells are similar except that the output of the second cell is 180^o phase shifted version of the first one during the steady state operation. Because of that, the theoretical background given in this section only covers the operation of the first converter and assumes that the extension of it to the second converter is straightforward. Also without loose of generality, it's assumed that the whole switching cycle is utilized by one converter.

As it is seen in Fig. 5(a), primary winding of the flyback transformer is connected to a dc source through a high frequency switch S. The switch is operated with period **T**. The duty cycle of the switch is given by **DT** where **D** is a real value between 0 and 1. At each period **T**, the switch **S** is **on** for the time length of **DT** and **off** for the duration of **(1-D)T**. There are 2 stages of operation for the converter in its steady state when the above described PWM signal is applied to the switch **S** which is illustrated schematically in Fig. 5.

a. Switch on Case

When switch S is **on**, the operation of the converter simplifies to the circuit given in Fig. 5(a). During this stage, the input dc source directly gives energy to the magnetizing inductance of the primary winding L_m. There is no current flowing through the secondary winding at this stage. This is due to the fact that the diode at the output is reverse biased because of the chosen dot notation of the transformer. The load is only fed by the output capacitor. Equations describing this stage of operation are as follows.

$$\frac{di_{Lm}}{dt} = \frac{1}{L_m}(V_s - i_{Lm}R_{on}) \quad (2)$$

$$\frac{dv_c}{dt} = \frac{-i_o}{C_o} \quad (3)$$

b. Switch off Case

The circuit schematic describing operation of the converter for this stage is given in Fig. 5(b). When the switch is **off**, the diode at the secondary side becomes forward biased. The stored energy in the magnetizing inductance from the previous stage causes current i_2 to flow through the secondary winding of the transformer. i_2 charges the output capacitor as well as provides energy demand of the load. Equations of interest for this mode of operation are given below.

$$\frac{di_{Lm}}{dt} = -\frac{(v_c + v_D)}{L_m N} \quad (4)$$

$$\frac{dv_c}{dt} = \frac{1}{C_o}\left(\frac{i_{Lm}}{N} - i_o\right) \quad (5)$$

D. The Output Filter and H Bridge Block

The output filter block provides a low pass filtering in order to remove high frequency harmonics from the output current. Since there are 2 switches each operated with 62 kHz frequency, harmonics at the output waveform are located at 124 kHz or more. This allows the filtering of harmonics to be accomplished easily with small valued passive circuit parts. For proper operation of the low pass filter, the corner frequency of the low pass filter could be placed at 12.4 kHz or lower. The outputs of this block are full wave rectified waveforms for both the output voltage and current signals. The H Bridge block is used to convert the shape of these signals into sinusoidal ac waveforms of 50 Hz. The H bridge block is implemented with 4 switches that are oriented as full wave rectification circuit.

E. PLL Block

The ac waveforms at the output of the H bridge block are processed by the PLL block for the purpose of grid integration. The block diagram of the PLL implementation is given in the Fig. 6.

F. The Control System Block

The block diagram of control structure of the developed grid connected micro inverter system is given in the Fig. 7. The main control objective that has to be accomplished by the control algorithm is to control

output current i_o in order to obtain full wave rectified sinusoidally shape current signal. A PI controller is utilized for this purpose.

In order to implement this control objective, the transfer function between output current i_o and the modulation input **D** (duty cycle) needs to be obtained. This can be accomplished by means of state space averaging method. The state space model of the converter needed for this method is obtained by using the systems state equations described in the section C. Using those formulas, the transfer function between the i_o and the **d** is calculated as:

$$\frac{I_o(s)}{d(s)} = \frac{-1.225x10^{10}s+1.798x10^{15}}{s^3+7950s^2+6.459x10^9s+4.058x10^{12}} \quad (6)$$

which can be used to perform small signall analysis of the converter. The values of the parameters in the state space model are given in the Table II. As it is seen, the transfer function has one right half zero which is typical for this converter type. All 3 of its poles are at left half plane which indicates that the open loop system is stable. The Bode plots of the transfer function are given in the Fig. 8.

The Fig. 8 shows that gain and phase margins of the system are − 32.1 dB and − 132^o which indicates that the system would need a controller during the closed loop operation.

Implementation of a PI controller would ensure stable operation of the converter while obtaining output current i_o of 100 Hz full wave rectified sinusoidal signal with low harmonic distortion. The Bode plot of the control loop with PI compensator is given in the Fig. 9. The Fig. 9 shows that the systems gain and phase margins are improved to 4.42 dB and 96.7^o which indicates that the closed loop system with the implemented PI controller is stable.

It can also be seen from the Fig. 9 that the systems gains at operating frequency of 100 Hz (rectified signal frequency for 50 Hz) and switching frequency of 62 kHz are 16.3 dB and − 15 dB respectively. The K_p and K_i parameters of the PI controller are obtained heuristically and shown in Table I.

Table I. Calculated values of PI controller parameters

PI Controller	Kp	Ki
PI	0.015	0.01

The above described control structure is implemented in the developed Simulink program with the Control System block which is shown in Fig. 10.

III. Matlab/Simulink Program

In order to simulate behavior of the above described microgrid system, several Matlab scripts and a simulink program are developed. The Matlab scripts are mainly used for purposes such as parameter

calculations and/or optimization and tuning of those values. Once these stages are completed, the obtained values are substituted into the Simulink model in order to perform simulation of the whole

system. Figure 11 shows the main module of the developed Simulink program. Figure 12 shows one of the Flyback converter implementation of the interleaved structure named Flyback1 as a sub-system. Table II shows specifications for the PV panel, interleaved flyback converter and other parameter values used during the design phase of the system.

Table II. Specifications for the PV panel, interleaved flyback converter and other parameters.

PV PANEL DESIGN PARAMETERS		FLYBACK CONVERTER DESIGN PARAMETERS	
Open Circuit Voltage V_{oc} (V)	37,6	Input Voltage (V)	29,74
Short Circuit Current I_{sc} (A)	8,6	Output Voltage (V)	220
Maxsimum Power Point Voltage V_{mp} (V)	29,74	Switching Frequency (Hz)	62000
Maxsimum Power Point Current I_{mp} (A)	8,1	Magnetizing Inductance Lm (µH)	12.8
βV_{oc} (%)	-0,35	Output Capacitor C_o (µF)	2
αI_{sc} (%)	0,06	Transformer Turn Ratio N	8
Ns	60	Duty Cycle (D)	0.48
Np	1	Input Voltage ripple (%)	1
Power (Watt)	250	Decoupling Capacitor C_{Decup} (mF)	86

IV. Sımulatıon Results and discussions

Before running the developed simulation program, a preliminary study should be done in order to find or optimize some system parameters and circuit element values. Some of the parameter values that have to be obtained with this preliminary study are the magnetizing inductance value that enable the flyback transformer to operate in CCM operating mode, the decoupling capacitor value corresponding to the desired panel output voltage ripple, the output capacitor value corresponding to the desired output current ripple of the converter and the duty cycle value corresponding to the steady state operation of the system for the adjusted switching frequency. Some of these parameter values were shown in the Table II. After calculating these parameter values, the state space model of the system was obtained. Using the state space averaging method, transfer function from the output current to the duty cycle was found in order to be used in the small signal analysis of the system. Finally, the determination of the

PI controller parameter values was done. Once the parameter calculation and initialization stage is completed, the developed simulation program is started. Graphical visuliation of selected parameter values are demonstrated in the following figures. The top figure in the Fig. 13 shows reference signal for the grid current versus the sinusoidaly shaped converter output capacitor current. The botom figure in the Fig. 13 gives reference signal for the grid voltage versus the sinusoidaly shaped converter output capacitor voltage. The signals belonging to the converter are shown after they are being processed by the output filter. In the figures the converter output signals are shown with a blue color while the reference signals are shown with a red. Converter output voltage and current signals are those that are connected to the grid by means of the PLL block after rectification and filtering operations. Figure 14 dispalys magnetizing current signals for flyback 1 and the flyback 2 converters. Figure 15 shows decoupling capacitor voltage.

From the Fig. 13, it's clear that both voltage and the current signal at the output of the H bridge block are sinusoidal in shape and 50 Hz in frequency. The THD of the grid current is calculated as 11.57% due to the spikes at the zero crossings. From the Fig. 14, it's seen that magnetizng current signals of the interleaved flyback architecture cause the grid current to have harmonic content at frequency 124 kHz. The peak to peak variation of one of the interleaved flyback output current is approximatly 21 A. Figure 15 gives the voltage seen on the decoupling capacitor. There is a peak to peak ripple voltage of around 1.5 V on the decoupling capacitor voltage which mainly causes the THD of the output current.

V. CONCLUSION

In this work, a simulation study of grid connected micro inverter is performed which uses an interleaved flyback topology. The input source for the micro grid is obtained from a PV panel. Two flyback converters are utilized in interleaved architecture operating in the CCM mode. The output of the converter is first converted into sinusoidal ac signal waveform by an H bridge block and then connected to the grid by means of a PLL block. A PI controller is implemented in order to achieve proper control of the system. Several programs are developed in Matlab and Simulink to find and optimize values of the design parameters such as the value of magnetizing inductance L_m, the value of decoupling capacitor C, values of K_p and K_i parameters of PI controllers etc. Simulation results demonstrated that the developed system successfully obtained ac voltage and current signals at 50 Hz in frequency and 220 V rms in amplitude. The THD of the grid current is found as 11.57% due to spikes at zero crossings.

Declarations

Ethical Approval: Not Applicable

Competing interests: The author declares that he has no conflict of interest in regard to this work with any people or institutions.

Authors' contributions: Not Applicable

Funding: Not Applicable

Availability of data and materials: Values of data used in the simulations are specified in the manuscript.

References

1. S. Barua and B. Billah “Promoting Sustainable Development: Solar Energy for the Urban Building Application,” International Conference on Mechanical Engineering and Renewable Energy ISSN: 2221-2213, At Chittagong University of Engineering Technology, Bangladesh, 2015. DOI: 10.13140/RG.2.1.1369.8640
2. S. B. Kjaer, J. K. Pedersen, F. Blaabjerg, “A review of single-phase grid-connected inverters for photovoltaic modules,” IEEE Trans. Ind. Appl., vol. 41, no. 5, pp. 1292–1306, Sep. 2005. DOI: 10.1109/TIA.2005.853371
3. Y. Li and R. Oruganti, “A low cost flyback CCM inverter for AC module application,” IEEE Trans. Power Electronics, vol. 27, no. 3, pp. 1295–1303, Mar. 2012.DOI: 10.1109/TPEL.2011.2164941
4. Y.H. Kim, J. G. Kim, Y. H. Ji, C. Y. Won, T. W. Lee, “Flyback inverter using voltage sensorless MPPT for AC module systems”, International Power Electronics Conference (IPEC), 2010, pp. 948-953, 2010.DOI: 10.1109/IPEC.2010.5543650
5. H. Hu, S. Harb, N. H. Kutkut, Z. J. Shen, and I. Batarseh, “A single-stage microinverter without using electrolytic capacitors,” IEEE Trans. Power Electron., Vol. 28, No. 6, pp. 2667–2687, Jun. 2013.DOI: 10.1109/TPEL.2012.2224886
6. N. Kasa, T. Iida, and L. Chen, “Flyback inverter controlled by sensorless current MPPT for photovoltaic power system,” IEEE Trans. Ind. Electron., Vol. 52, No. 4, pp. 1145–1152, Aug. 2005.DOI: 10.1109/TIE.2005.851602
7. S. Zengin, F. Deveci, M. Boztepe, “Decoupling capacitor selection in DCM flyback PV microinverters considering harmonic distortion,” IEEE Trans. Power Electronics, Vol. 28, No. 2, pp. 816–825, Feb. 2013.DOI: 10.1109/TPEL.2012.2203150
8. N. D. Benavides, P. L. Chapman, “Modeling the effect of voltage ripple on the power output of photovoltaic modules,” IEEE Trans. Ind. Electronics, Vol. 55, No. 7, pp. 2638–2643, June 2008.DOI: 10.1109/TIE.2008.921442
9. T. Esram and P. L. Chapman, “Comparison of photovoltaic array maximum power point tracking techniques,” IEEE Trans. Energy Conversion, vol. 22, no. 2, pp. 439–449, June 2007.DOI: 10.1109/TEC.2006.874230
10. M. Gao, M. Chen, Q. Mo, Z. Qian, Y. Luo, “Research on output current of interleaved-flyback in boundary conduction mode for photovoltaic AC module application”, IEEE 2011 Energy Conversion Congress and Exposition (ECCE), pp. 770-775, 2011.DOI: 10.1109/ECCE.2011.6063848
11. G. H. Tan, J. Z. Wang, Y. C. Ji, “Soft-switching flyback inverter with enhanced power decoupling for photovoltaic applications”, Electr. Power Appl., Vol. 1, no. 2, pp. 264–274, Mar. 2007.DOI: 10.1049/iet-epa:20060236

12. N. P. Papanikolaou, E. C. Tatakis, “Active Voltage Clamp in Flyback Converters Operating in CCM Mode Under Wide Load Variation”, IEEE Trans. Ind. Electronics, Vol. 51, No. 3, pp. 632–640, June 2004.DOI: 10.1109/TIE.2004.825342
13. Li Yanlin, R. Oruganti, "A low cost high efficiency inverter for photovoltaic ac module application", Photovoltaic Specialists Conference (PVSC), pp. 002853-002858, 2010.DOI: 10.1109/PVSC.2010.5615940
14. P. D. Maycock, "Cost reduction in PV manufacturing: impact on grid-connected and building integrated market", Solar Energy Mater. Solar Cells, vol. 47, no. 1–4, pp. 37-45, Oct. 1997.https://doi.org/10.1016/S0927-0248(97)00022-6
15. Kyritsis A. Ch, E.C. Tatakis, N.P. Papanikolaou, Patras Univ. Patras, "Optimum design of the current-source flyback inverter for decentralized grid-connected photovoltaic systems", IEEE Transactions on Energy Conversion, vol. 23, no. 1, pp. 281-293, March 2008.DOI: 10.1109/TEC.2007.895854
16. S. B. Kjaer, F. Blaabjerg, "Design optimization of a single phase inverter for photovoltaic applications", Proc. IEEE PESC'03, vol. 3, pp. 1183-1190, 2003.DOI: 10.1109/PESC.2003.1216616
17. T. Shimizu, K Wada, N. Nakamura, "Flyback-type single-phase utility interactive inverter with power pulsation decoupling on the dc input for an ac photovoltaic module system", IEEE Transactions on Power Electronics, vol. 21, no. 5, pp. 1264-1272, Sep. 2006.DOI: 10.1109/TPEL.2006.880247
18. Gu Jun-yin, Wu Hong-fei, Chen Guo-cheng, Xing Yan, "Research on photovoltaic grid-connected inverter based on soft-switching interleaved flyback converter", IEEE Conference on Industrial Electronics and Applications, pp. 1209-1214, 2010.DOI: 10.1109/ICIEA.2010.5515610
19. B. Tamyurek, B. Kirimer, “An Interleaved Flyback Inverter for Residential Photovoltaic Applications”, Proc. of 15th Europeon Conference on Power Electronics and Applications, pp. 1–10, 2013.DOI: 10.1109/EPE.2013.6634424
20. B. Tamyurek, B. Kirimer, “An Interleaved High-Power Flyback Inverter for Photovoltaic Applications”, IEEE Transactions on Power Electronics, Vol. 30, No. 6, June 2015 DOI: 10.1109/TPEL.2014.2332503
21. Jason Arrigo, " Input and Output Capacitor Selection," Application Report, SLTA055, Texas Instruments,2006
22. J. Cubas, S. Pindado, M. Victoria. “On the Analytical Approach for Modeling Photovoltaic Systems Behavior”, Journal of Power Sources, Vol 247, pg 467–474, 2014 DOI: 10.1016/j.jpowsour.2013.09.008
23. M. Frankiewicz, A. Gołda, A. Kos. “Design and tests of CMOS phase locked-loop”, Proceedings of the 18th International Conference Mixed Design of Integrated Circuits and Systems, Gliwice, Poland pp. 295 - 298, 2011.
24. Grid-Connected Solar Microinverter Reference Design, Microchip Technology Inc., U.S.A, 2012, pp. 36–38.
25. Hart, Daniel W. DC Power Supplies, Power Electronics. 2nd Edt. In: McGraw Hill Publication, New York, USA, 2011; 265-330.

26. Zengin S., Deveci F., Boztepe M., 2013, Decoupling Capacitor Selection in DCM Flyback PV Microinverters Considering Harmonic Distortion, IEEE Transactions on Power Electronics, Vol 28, No 2, pp 816-825.
27. Aldwihi B.A, Salihmuhsin M., “Modeling of Photovoltaic Panels Using Matlab/Simulink”, Kahramanmaras Sutcu Imam University Journal of Engineering Sciences, Vol 22, No 2, pp 78-87, 2019.
28. Isler Y. S., Salihmuhsin M., Categorization of Software Tools for Renewable Energy Sources, International Conference on Natural Science and Engineering (ICNASE’16), March 19-20, Kilis, Turkey, 2016
29. Isler Y. S, Yilmaz S., Salihmuhsin M., İstanbul Şartlarında 10 kWp Optimum Verimli Fresnel Parabolik Oluk Tipi Güneş Kolektörü Tasarımı ve Maliyet Analizi, International Conference on Renewable Energy Technologies and Applications (RETA'16), p 1-9, March 5-6, Istanbul, Turkey, 2016
30. Isler Y. S., Salihmuhsin M., Stand-Alone Photovoltaic Systems for Telecommunication Stations, a Case Study for Kahramanmaras, Turkey. International Journal of Scientific and Technological Research, Vol:4, Issue: 8, p 138-146, 2018
31. Isler Y. S., Salihmuhsin M., Şebekeden Bağımsız PV Sistemin TRNSYS ile Gerçek Zamanlı Modellenmesi, Kahramanmaras Sutcu Imam University Journal of Engineering Sciences, Vol: 21, Issue: 1, p 66-76, 2018
32. Isler Y. S., Salihmuhsin M., Performance Analysis of Storage, Grid Connected Hybrid Photovoltaic System, International Scientific and Vocational Journal , Vol:2, Issue: 2, p 118-124, 2018
33. Isler Y. S., Salihmuhsin M., Depolamalı, Şebeke Bağlantılı Hibrit Fotovoltaik Sistemin Performans Analizi. II. International Scientific and Vocational Studies Congress, 2018
34. Isler Y. S., Salihmuhsin M., Azimut Açısının Güneş Enerjisi Santralinde Üretime Etkisini Modellenmesi ve Performans Analizi. II. International Scientific and Vocational Studies Congress, 2018
35. Isler Y. S., Salihmuhsin M., Güneş Enerjisi Santrallerinde Sehpa Seçiminin Performansa Etkisinin Analiz Edilmesi Ve Sıcaklık Etkisi. El-Cezeri Journal of Science and Engineering, Vol: 6, Issue: 1, p 97-107, 2019
36. Salihmuhsin M., (2022). Simulation of a Flyback Converter in Open Loop, 2.nd International Mediterranean Scientific Research and Innovation Congress, pp. 1072-1078
37. Salihmuhsin M., (2022). Farklı Aydınlanma ve Sıcaklık Koşullarında Çalışan Bir Güneş Paneli Simülatörü, 2.nd International Mediterranean Scientific Research and Innovation Congress, syf. 1064-1071
38. Salihmuhsin M., Durum Uzayı Ortalaması Metoduyla Bir Geri Dönüşlü Dönüştürücü İçin Küçük Sinyal Analizi, Uluslararası Mühendislik Bilimleri Kongresi, 11-12 Kasım, Baku, Azerbaycan Teknik Üniversitesi, 2022.
39. Salihmuhsin M., Simulation of Effect on Selecting decoupling Capacitor Voltage Value on the Output Power of a Flyback Converter Fed by a PV Panel, Kahramanmaras Sutcu Imam University Journal of Engineering Sciences, Vol 26, No 1, 2023.

Figures

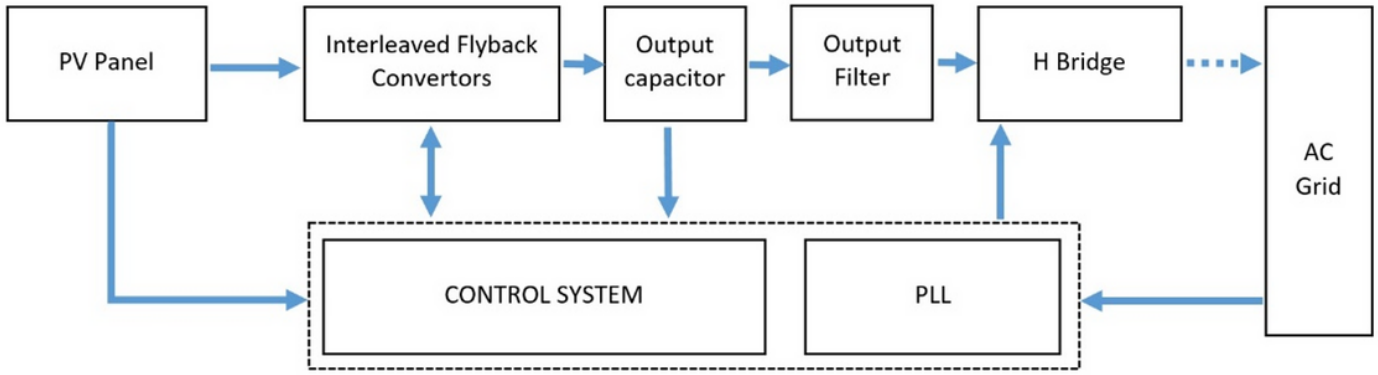

Figure 1

Block diagram of the grid connected micro inverter system.

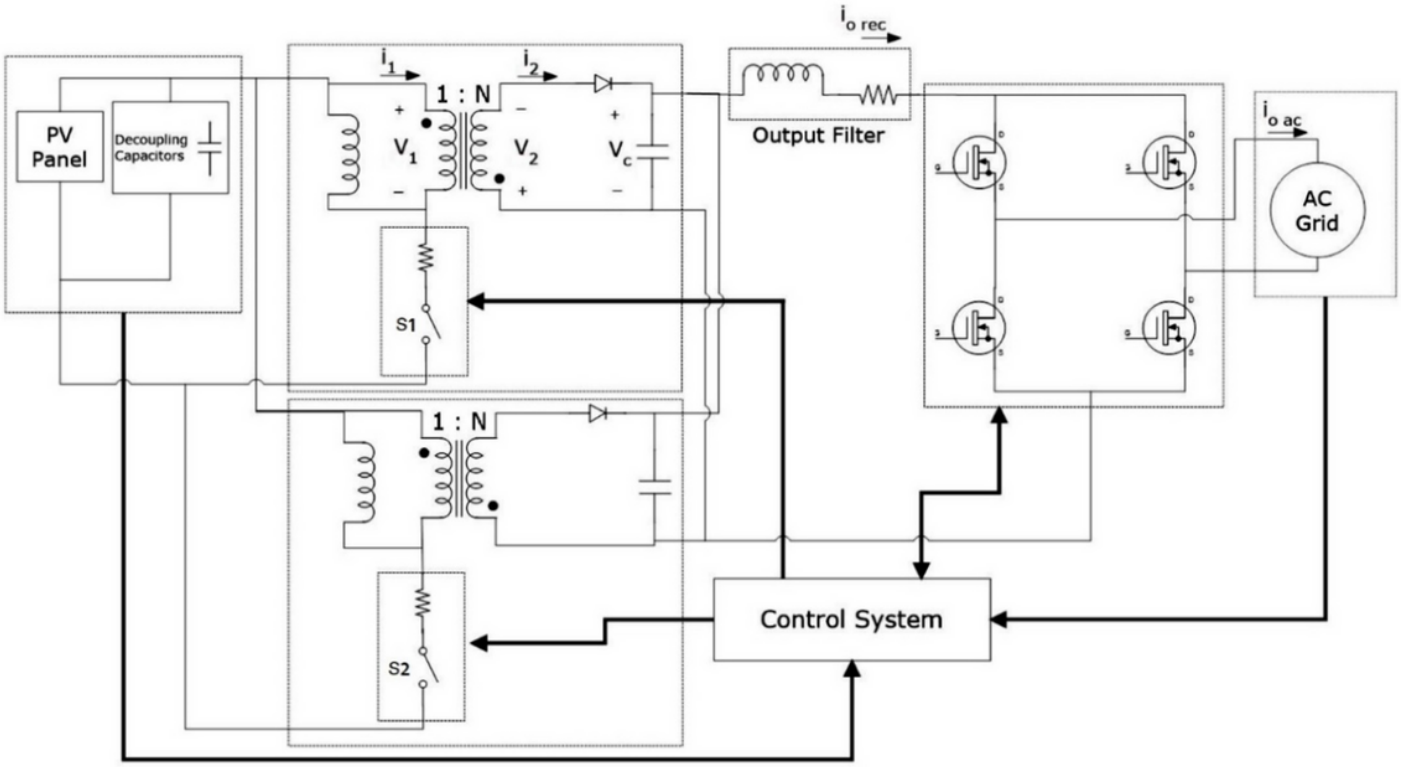

Figure 2

Circuit schematic of the proposed system

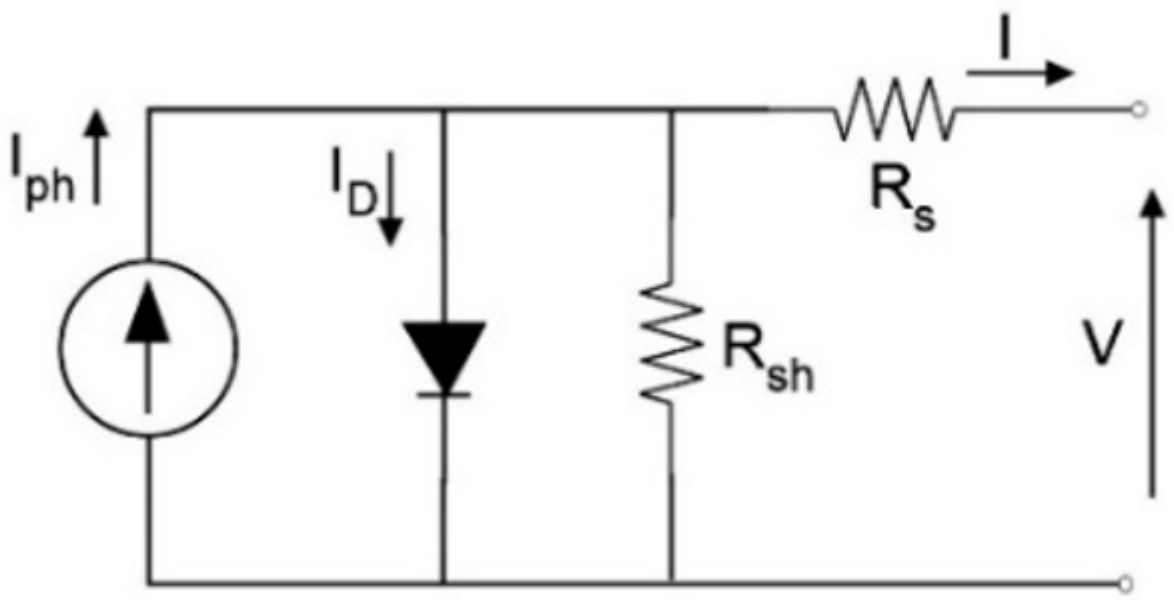

Figure 3

Circuit schematic of the PV cell used in modelling.

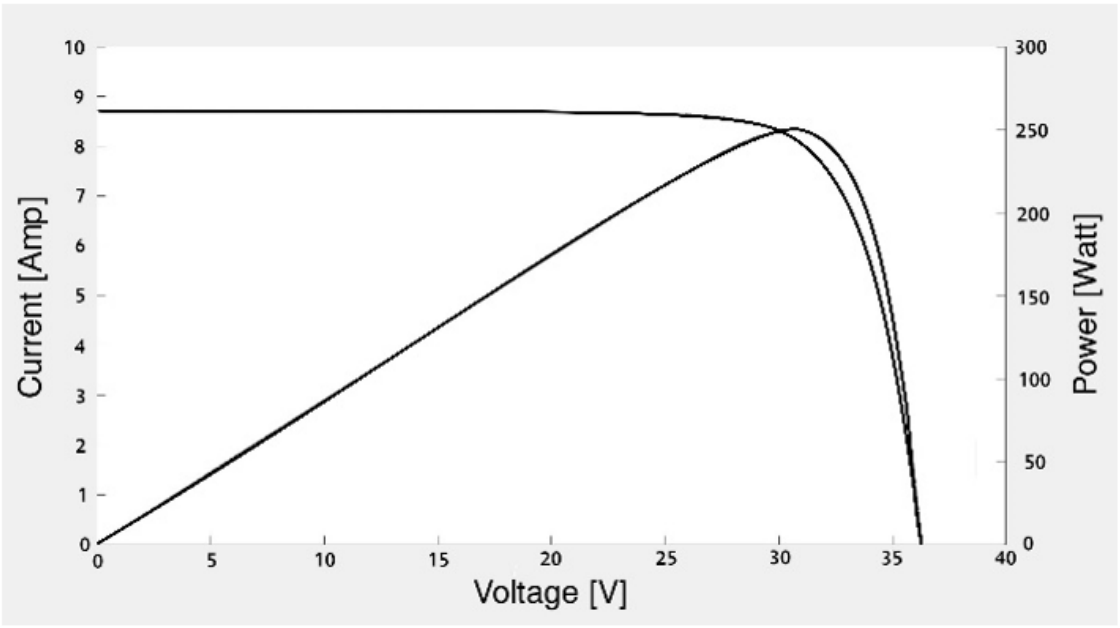

(a)

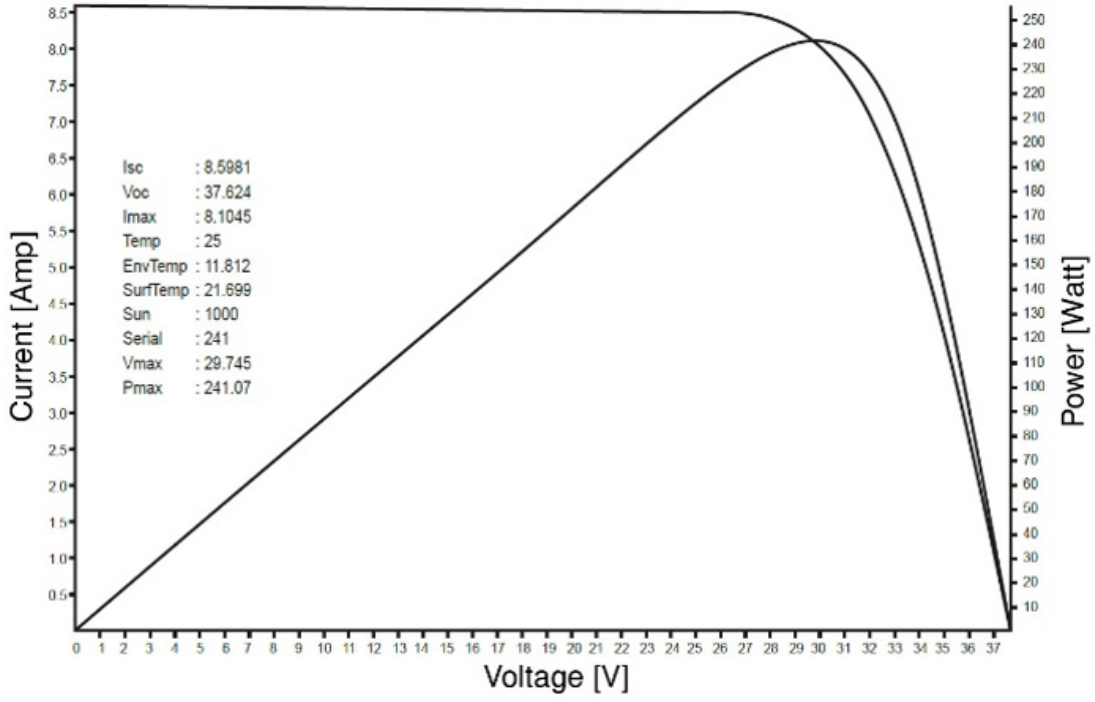

(b)

Figure 4

(a): I-V curve and P-V curve of the panel generated by the developed program at STC. (b): Corresponding curves provided by the manufacturer.

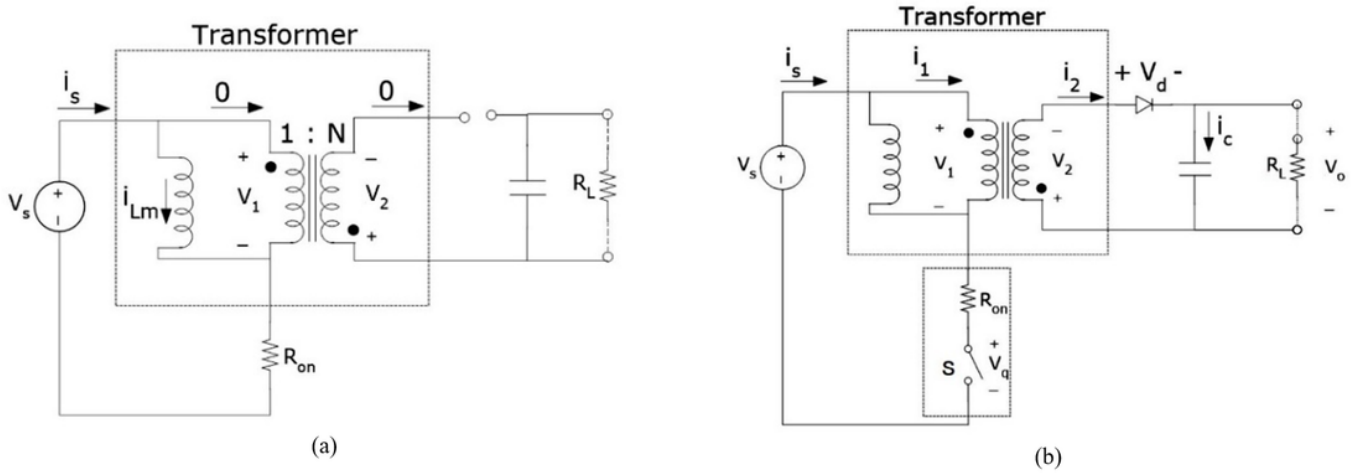

Figure 5

(a) Equivalent circuit of the flyback converter for the switch ***on*** case. (b) Schematic for the switch ***off*** case.

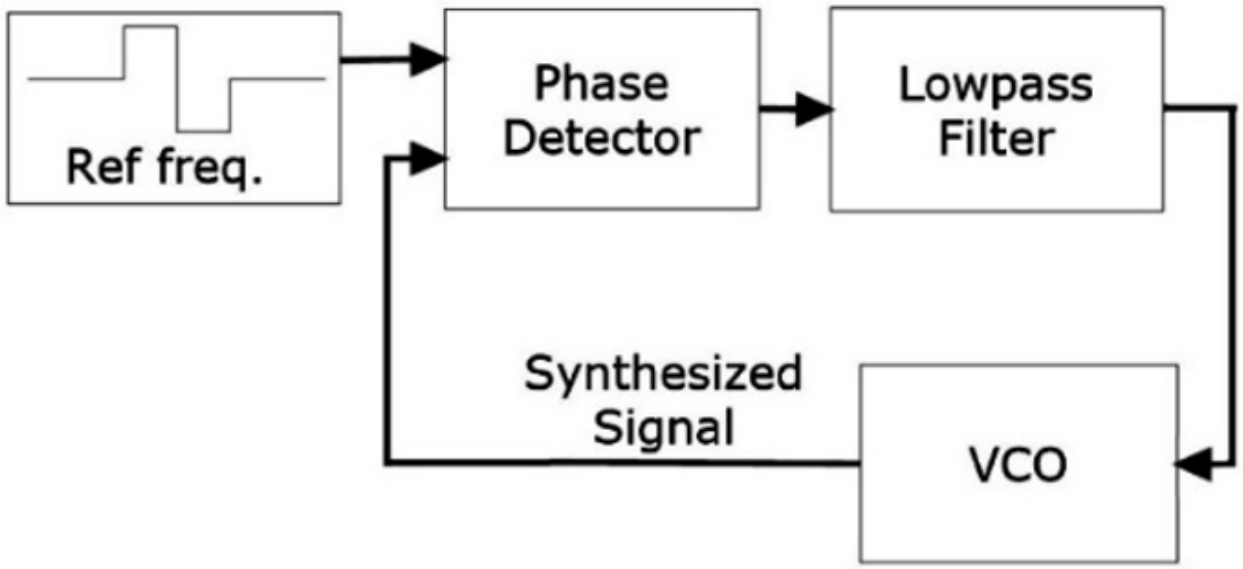

Figure 6

PLL block

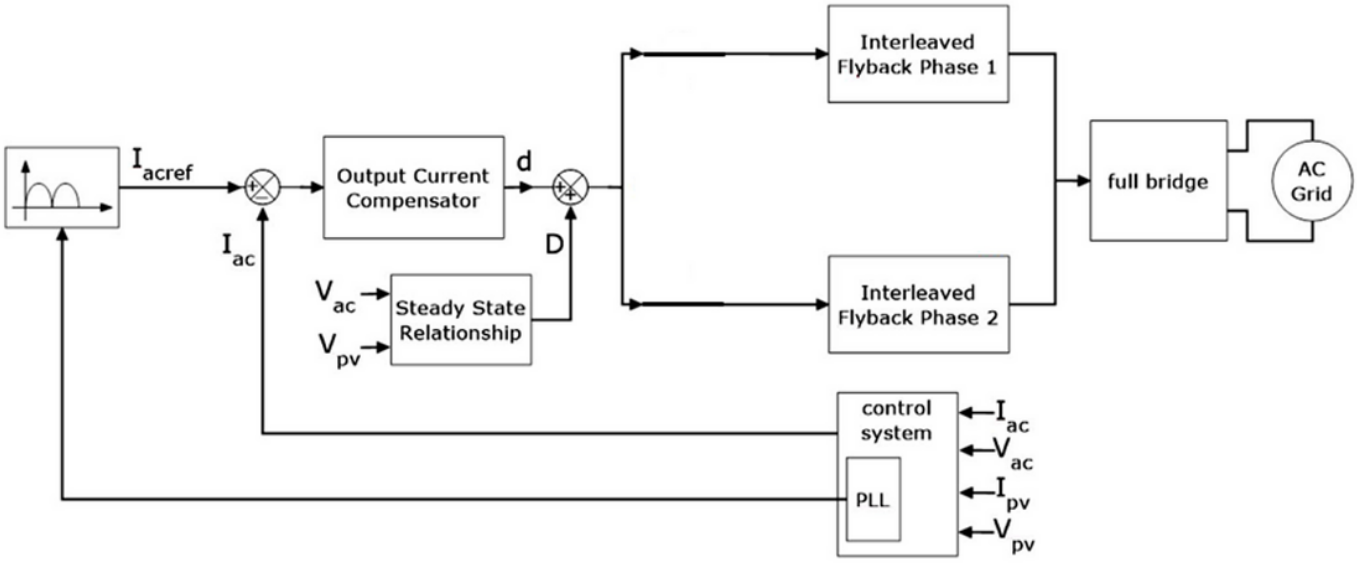

Figure 7

Block diagram of the control structure

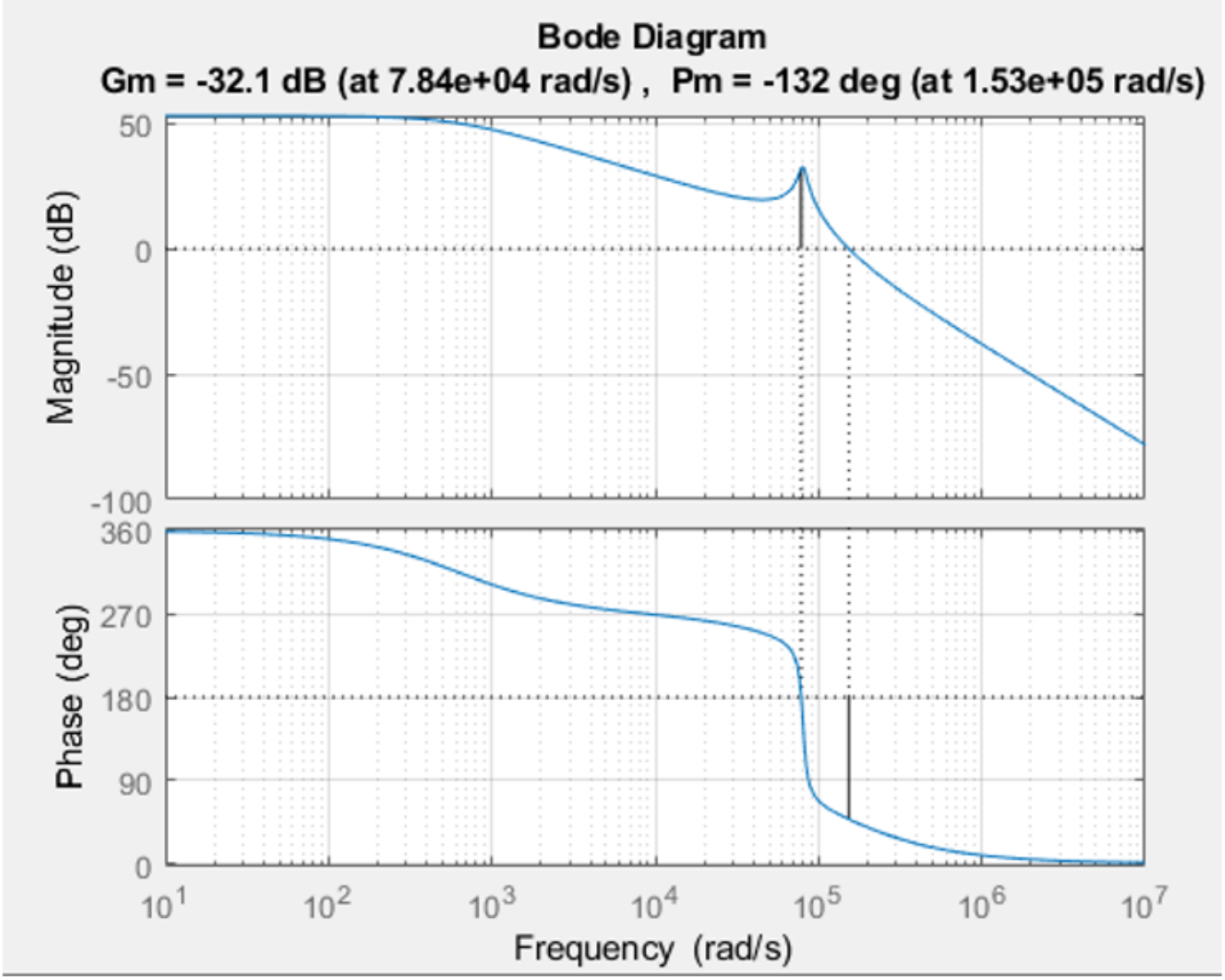

Figure 8

Bode plots of the transfer function

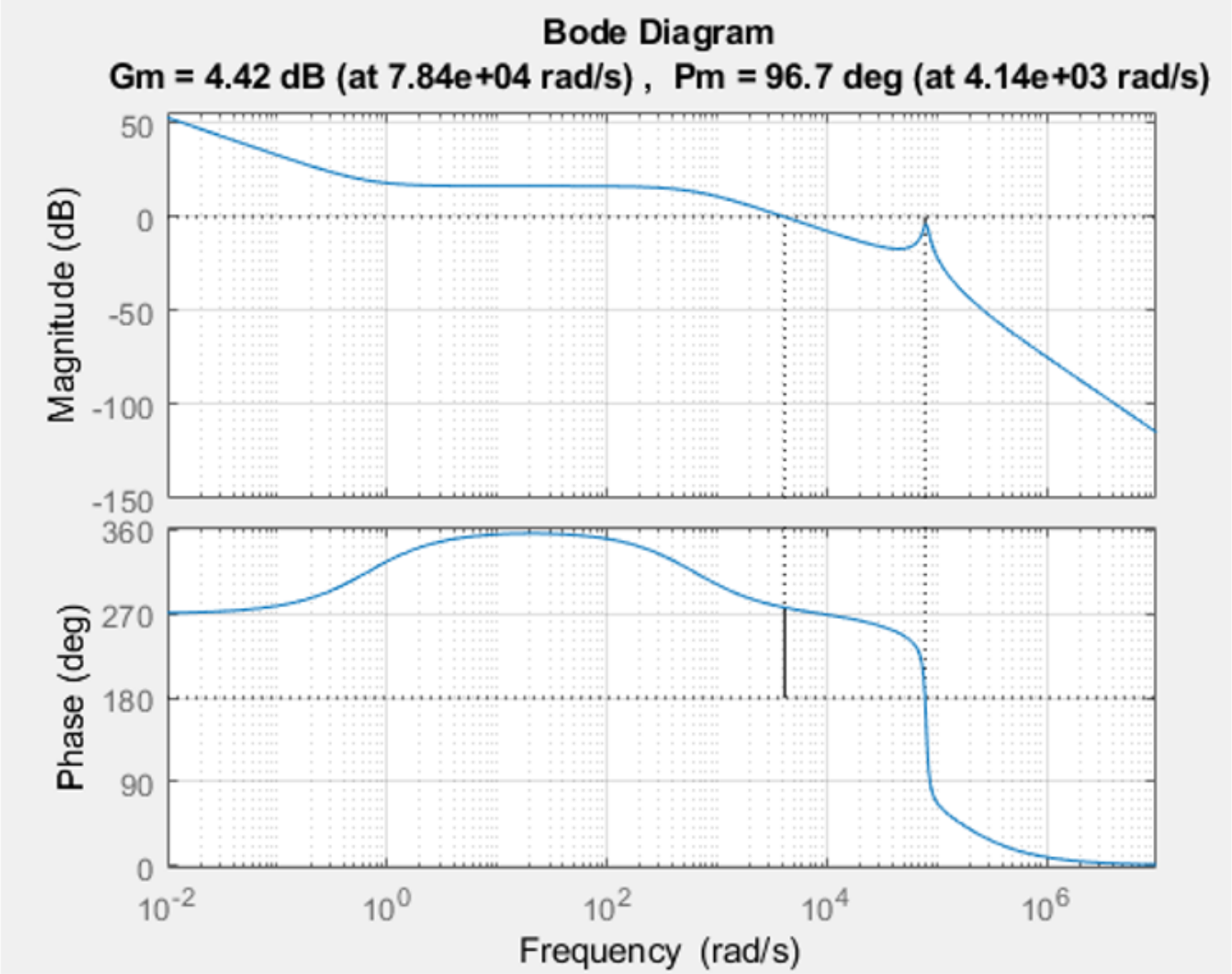

Figure 9

Bode plots of the transfer function with PI controller.

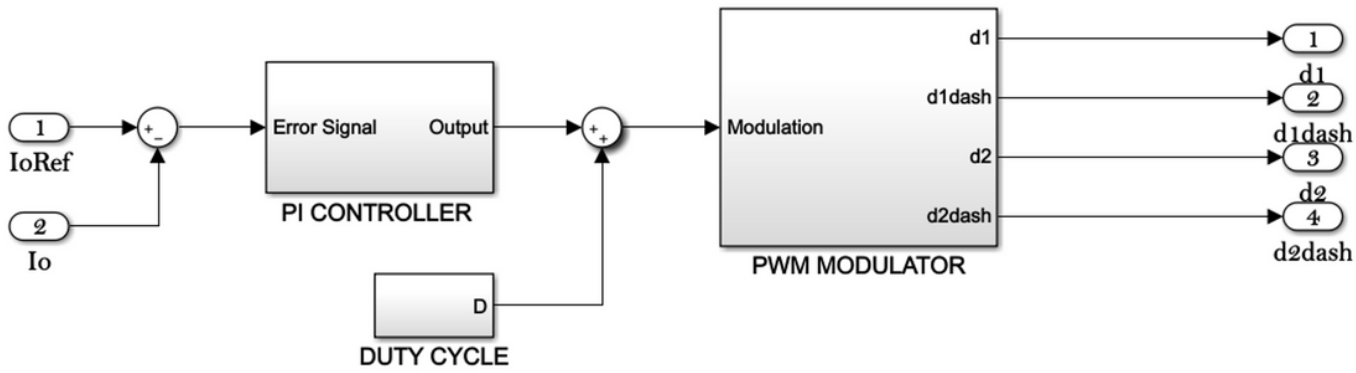

Figure 10

Control System block of the developed Matlab/Simulink program.

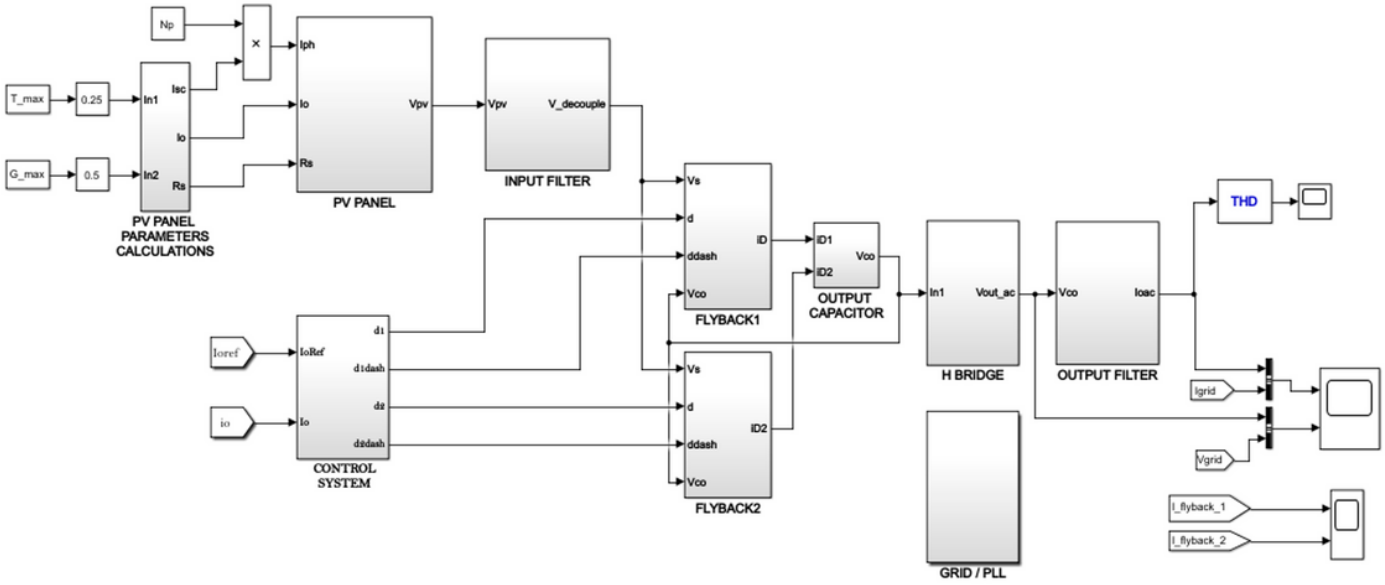

Figure 11

Developed Simulink implementation of the overall system

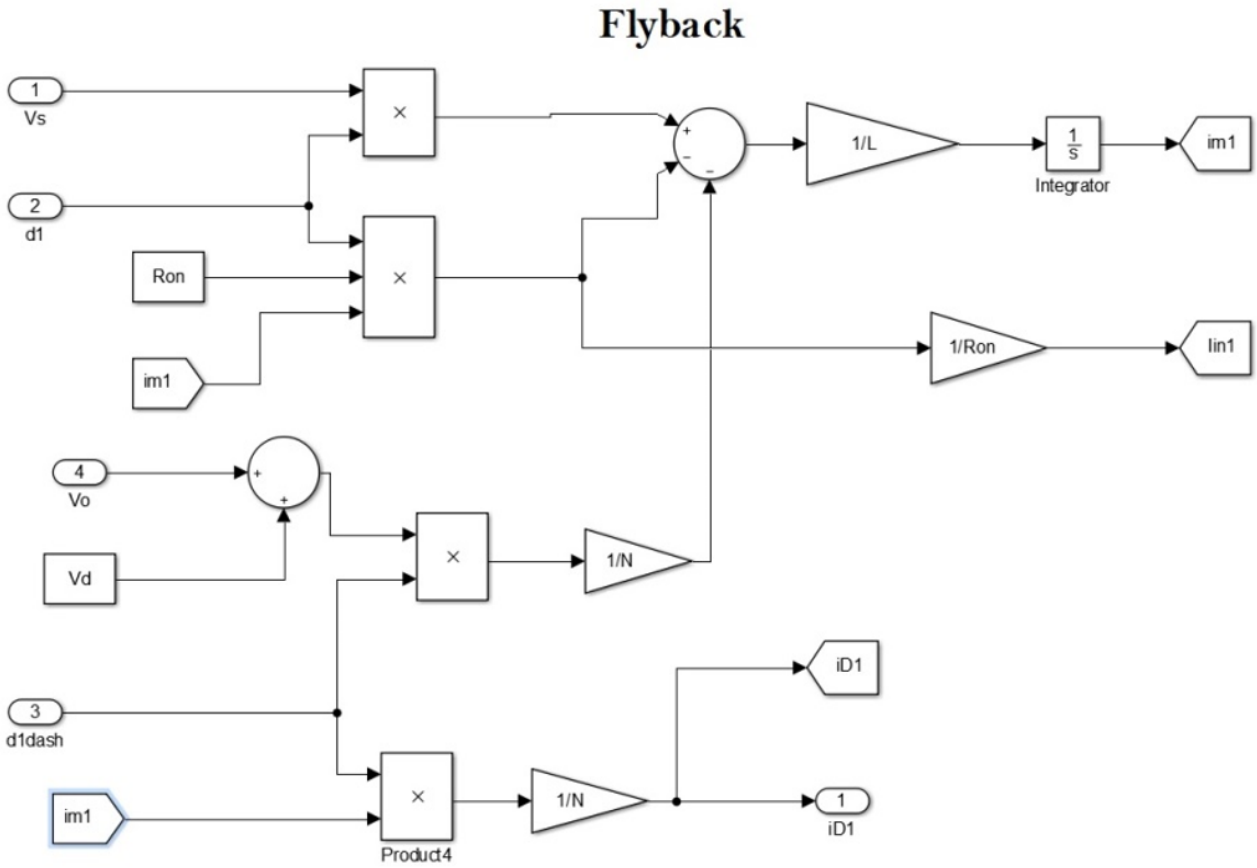

Figure 12

Simulink implementation of the FLYBACK1 sub system

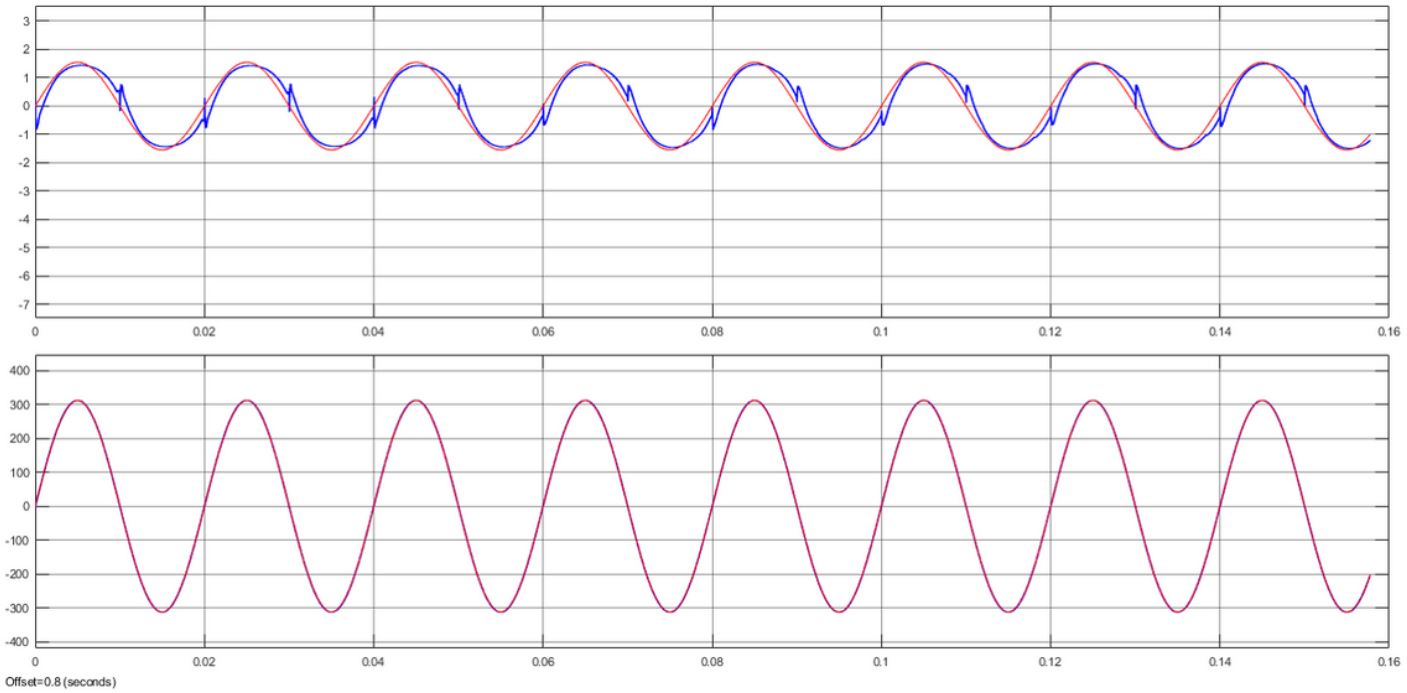

Figure 13

Simulation results for reference signal for the grid current versus the rectified converter output current (top figure) and reference signal for the grid voltage versus the rectified converter output voltage (bottom figure). Reference signals are shown in red.

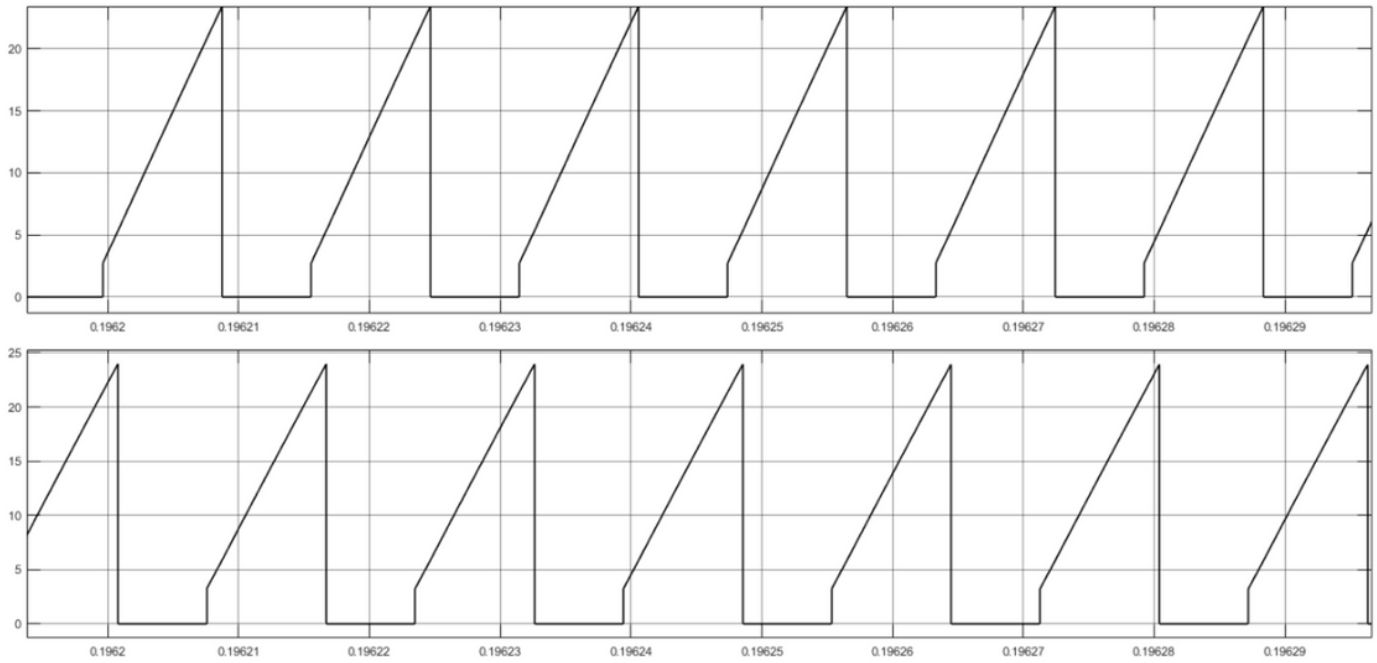

Figure 14

Signal waveforms of magnetizing currents for flyback 1 (top figure) and flyback 2 transformers.

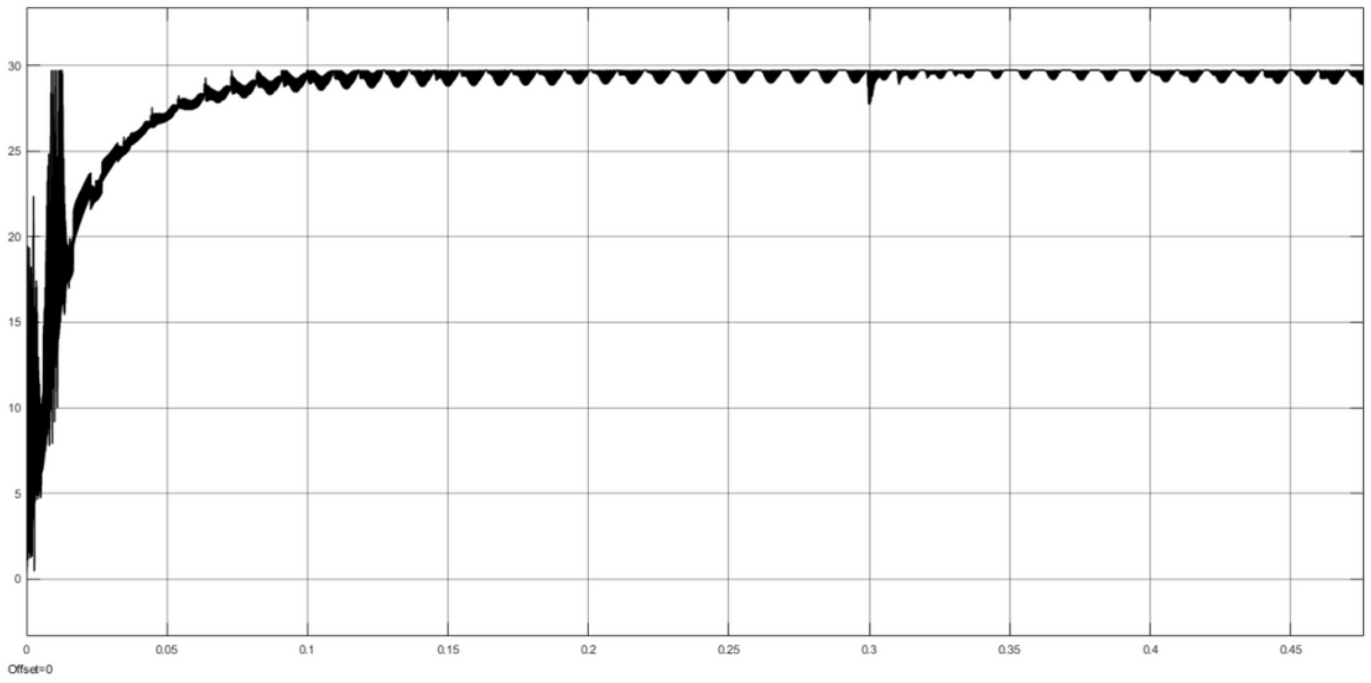

Figure 15

Signal waveform for decoupling capacitor voltage.